British Journal of Pharmacology (1996) 118, 1127-1140

Activation and cooperative multi-ion block of single nicotinic-acetylcholine channel currents of *Ascaris* muscle by the tetrahydropyrimidine anthelmintic, morantel

*A.M. Evans & [1]R.J. Martin

Department of Preclinical Veterinary Sciences, R.(D).S.V.S, University of Edinburgh, Summerhall, Edinburgh EH9 1QH

1 We have investigated activation and block, by the tetrahydropyrimidine anthelmintic, morantel, of nicotinic-acetylcholine receptor (AChR) currents in membrane vesicles isolated from somatic muscle cells of the nematode parasite *Ascaris suum*. Standard single-channel recording techniques were employed. Morantel in the pipette (6 nM to 600 μM), activated single nicotinic AChR currents.

2 Kinetic properties of the main-conductance state of morantel-activated currents were investigated in detail throughout the concentration range, 0.6 μM to 600 μM. Open-time distributions were best fitted by a single exponential. Mean open-times were slightly voltage-dependent, increasing from 0.9 ms at +75 mV to 1.74 ms at −75 mV in the presence of 0.6 μM morantel. At low concentrations, closed-time distributions were best fitted by the sum of two or three exponential components.

3 As the concentration of morantel was increased (100-600 μM), fast-flickering open channel-block was observed at positive potentials, even though morantel, a cation, was only present at the extracellular surface of the membrane. The block rate was dependent on morantel concentration and both block rate and duration of block increased as the potential became less positive. A simple channel-block mechanism did not explain properties of this block.

4 At negative potentials, as the morantel concentration increased, a complex block was observed. With increases in morantel concentration two additional gap components appeared in closed-time distributions: one was short with a duration (~13 ms) independent of morantel concentration; the other was long with a duration that increased with morantel concentration (up to many minutes). In combination, these two components produced a marked reduction in probability of channel opening (*Po*) with increasing morantel concentration. The relationship between the degrees of block and morantel concentration had a Hill coefficient of 1.6, suggesting the involvement of at least two blocking molecules. The data were analysed by use of a simple sequential double block kinetic model.

Keywords: *Ascaris*; morantel; nicotinic-channels

Introduction

The somatic muscle cells which line the body wall of the nematode parasite *Ascaris suum* have been shown to contract in response to acetylcholine (Baldwin & Moyle, 1949; Natoff, 1969). The contraction is associated with a depolarization of the muscle cells (Del Castillo *et al.*, 1963), which is mediated by a ligand-gated, non-selective cation channel (Martin, 1982; Harrow & Gration, 1985; Pennington & Martin, 1990). This channel therefore serves the same function as those in muscle and nerve in vertebrates, and has been classified as nicotinic (Toscano Rico, 1926; Baldwin & Moyle, 1949; Natoff, 1969; Rozhova *et al.*, 1980). However, the nicotinic-acetylcholine receptor (AChR) found in the somatic muscle cells of *Ascaris* is clearly a distinct subtype for which there are a number of selective agonists, including the imidazothiazoles like levamisole and the tetrahydropyrimidines like morantel, (for a review see Martin *et al.*, 1991). The selective agonists, levamisole and morantel, are frequently used for therapeutic purposes as anthelmintics to control nematode parasite infestations of both animals and man.

In an electrophysiological study of the effects of nicotinic AChR agonists on the somatic muscle cells of *Ascaris*, Harrow and Gration (1985) obtained bell-shaped concentration-conductance curves for the tetrahydropyrimidine morantel, while sigmoidal curves were obtained with acetylcholine and the imidazothiazole levamisole. They also observed that morantel but not levamisole produced a markedly non-linear current/voltage (*I/V*) plot under voltage-clamp. No conclusive explanation for the self-antagonism or non-linear *I/V* plots exhibited by morantel was obtained. Because of the therapeutic importance of morantel as an anthelmintic, additional investigation is required to provide an understanding of its actions.

In a recent study Robertson and Martin (1993a) found that the anthelmintic levamisole both activated and blocked single nicotinic AChR currents isolated from the somatic muscle cells of *Ascaris*, even though this compound exhibits no clear self-antagonism with respect to the macroscopic nicotinic AChR currents (Harrow & Gration, 1985). This may be explained by the fact that levamisole produced fast-flickering open channel-block, which was marked only at holding potentials more negative than the normal resting potential of the cell. A more extreme form of channel-block or additional effects may underline the self-antagonism observed with morantel.

In this investigation, we have examined the effects of morantel at single nicotinic AChRs found on somatic muscle of the parasitic nematode *Ascaris suum*. Morantel was found to activate as well as block single nicotinic AChR currents. The degree of block produced by morantel was marked. With positive holding potentials a fast-flickering open channel-block was observed; at negative potentials a complex block, showing positive 'cooperativity' and a marked concentration-dependent reduction in the probability of channel opening was observed. The block was described by using a simple sequential double block model. Preliminary accounts have been published in abstract form (Evans & Martin, 1992a,b; 1993a,b).

[1] Author for correspondence.
*Present address: Department of Pharmacology, Mansfield Road, Oxford OX1 3QT.

Methods

The preparation and some of the analytical methods have been described previously (Robertson & Martin, 1993a). Briefly, muscle membrane vesicles were prepared by collagenase treatment from the somatic muscle cells of the nematode parasite, *Ascaris suum*. These muscle vesicles were mounted in a bath under phase contrast and single channel currents recorded using cell-attached or isolated inside out patches (Hamill *et al.*, 1981). Morantel (6 nM – 600 μM), the anthelmintic agonist under study, was added to the patch-pipette solution.

Solutions

The bath solution used was (concentration in mM): CsCl 35, CsAcetate 105, $MgCl_2$ 2, EGTA 1, HEPES 10, pH adjusted to 7.2 with CsOH. All experiments were performed at room temperature (18 – 22°C). The pipette solution contained (concentration in mM): CsCl 140, $MgCl_2$ 2, HEPES 10, pH adjusted to 7.2 with CsOH.

The concentration of the sole conducting cation (Cs^+) was symmetrical with respect to the bath and pipette solutions, while the concentration of the main anion (Cl^-) was non-symmetrical. Thus the morantel-activated single-channel currents, carried by the non-selective cation channel of the nicotinic-acetylcholine receptor (nAChR), could be identified by their reversal potential (0 mV).

Data analysis

Open- and closed-times To enable analysis of the kinetics of the single-channel currents activated by morantel, tapes of experimental records were replayed through an 8 pole Bessel filter (−3dB, 1.5 kHz), digitized every 70 μs (CED 1401 lab. interface) and stored in a data file on the hard disc of an IBM 386 (PS/2, model 70) via the PAT V6.1 single-channel analysis program (J. Dempster, Department of Physiology and Pharmacology, Strathclyde University). The system rise time and dead time were 0.22 ms and 0.14 ms, respectively. For the present study data were accepted for analysis when the activity of only a single channel was apparent, i.e. when no multiple openings were observed in the entire experimental record (> 5 min). The initial stages of the analysis were performed by use of the PAT V6.1 software. Single-channel current amplitude distributions were determined by constructing point amplitude histograms from a running average of the digitized record according to the methods of Patlak (1988). The open channel amplitude distributions were fitted by the sum of one or more Gaussian components by use of the Dempster software.

Transitions between open- and closed-states were determined by setting a threshold at approximately 75% of the current amplitude of the main-conductance state. In order to eliminate interference from openings to an apparent subconductance state, each event was then observed and edited appropriately, i.e. those closures which did not clearly enter the subconductance state and did not approach 50% of the main conductance state amplitude were designated open. As transitions to the subconductance state were very rare (see results), it was assumed that the gating kinetics of the main conductance state were independent of the subconductance openings. Thus for the purposes of this study all openings to the subconductance state, and all transitions to this state from the main conductance state were defined as closed. Edited files of open- and closed-times were compiled and stored on floppy disc. These data files were then transferred to the Edinburgh University VAX-11/780 main frame computer system for further analysis. A minimum resolvable interval, $t_{min} = 0.42$ ms, (for data filtered at 1.5 kHz) and maximum resolvable interval t_{max}, equal to the duration of the recording, was then imposed on the data and a conditional probability function of the form:

$$\text{p.d.f.} = \frac{\sum_{i=1}^{k} \frac{a_i}{\tau_i} \cdot e^{-t/\tau_i}}{\sum_{i=1}^{k} a_i \left(e^{-t_{min}/\tau_i} - e^{-t_{max}/\tau_i}\right)} \quad (1)$$

fitted to the open- and closed-times by the method of maximum likelihood (Colquhoun & Sigworth, 1983, p. 245) with the help of the NAG minimizing subroutine, E04CCF. In the p.d.f., a_i represents the area of the i^{th} component ($\sum a_i = 1$), τ_i is the time constant or mean value of the i^{th} component, t represents time and k equals the number of exponential terms fitted. In general the sample length was 70 s. However, for experiments where the probability of opening was low due to channel-block (concentrations ⩾ 100 μM morantel, at negative holding potentials), the sample time had to be extended up to 4 min in order to record enough events for analysis. The apparent mean open- and closed-times were estimated by the summing of the relative area of each exponential component multiplied by the time constant of that component.

Bursts were defined as single openings or groups of openings separated by the shortest gap component or closures that occur (Colquhoun & Sigworth, 1983; Colquhoun & Sakmann, 1985). Thus for the purposes of burst analysis a critical time (t_{crit}) was determined numerically (Robertson & Martin 1993a) for each data set. All closed-times with a duration less than t_{crit} were defined as those being within a burst of openings, while all closures with a duration greater than t_{crit} were defined as those with separate bursts.

Blockage duration and frequency at positive potentials The duration of the block, that produced a fast-flickering channel-block at positive potentials, was similar to the short 'within-activation' closures so an accurate measure of their duration and frequency was only made when the frequency of block was high relative to the frequency of the 'within-activation' closures. Thus the duration of block was taken as the short time constant (τ_1) from the closed-time distribution at concentrations greater or equal to 100 μM, the concentration at which the mean open-time of the morantel-activated currents began to decline.

Blockage frequency Plots of blockage frequencies were constructed for high concentrations of morantel at positive potentials from estimates of the total corrected number of blockages in the records and the total corrected open-times. The technique of Colquhoun and Sigworth (1983, p.246) for estimating the corrected number of events with a particular probability density function and value of t_{crit} was used: the number of blockages was taken as the corrected total number of short closings (time constant τ_1) assumed to be blockages under these conditions (see results). The technique of Colquhoun and Sakmann (1985, p.505) for estimating the corrected total open-time was used: this method corrects for missed events; it calculates the total time spent in gaps within bursts (m_{TS}), including those undetected; it calculates the total time occupied by bursts ($N_b m_b$) and determines the corrected total open-time from the difference ($N_b m_b - m_{TS}$). The corrected number of blockages (short closing) per corrected open time was then obtained.

Drugs

Morantel was a gift from Pfizer, Sandwich, U.K.

Least squares estimation

Non-linear least squares estimates were obtained with programs written in FORTRAN and run on the Edinburgh VAX-11/780 mainframe. The NAG subroutine E04CCF which minimizes functions specified by the user and utilizes the simplex method was employed.

Results

When added to the pipette solution, morantel activated single non-selective cation channel currents in membrane patches of vesicles isolated from the somatic muscle cells of *Ascaris suum*; no such events were observed in the absence of an agonist of the nAChRs ($n=84$). The conductance and kinetics of activation of these currents are similar to those described for acetylcholine- and levamisole-activated single-channel currents (Pennington & Martin, 1990; Robertson & Martin, 1993a). The concentration-dependence of activation of these nicotinic-acetylcholine receptor currents (nAChR) has been studied in relation to other agonists (Robertson & Martin, 1993a) and will not form part of this investigation, which will focus on the properties of the channel-block produced by morantel.

Morantel-activated currents have multiple conductance states

Single-channel conductance values showed substantial variation when individual current amplitudes were compared and it became clear that at least two open channel conductance states were activated by morantel (6 nM–600 μM). Figure 1a shows examples of the two current amplitudes commonly observed under a holding potential of −50 mV. These two states were clearly resolved within the amplitude histogram shown in Figure 1b. In addition to the main state peak at −2.5 pA, a secondary peak was detected at −2.0 pA; each was fitted well by a single Gaussian distribution. Although rare, transitions between the two conductance states were observed (Figure 1c). However, in general the open channel noise was virtually indistinguishable from that of the closed channel noise, and openings to each conductance state appeared to be discrete and independent events.

Both main- and sub-conductance states exhibit inward rectification

Figure 2a shows examples of single-channel openings to the main conductance state, as recorded from an excised inside-out patch in the presence of 6 μM morantel and a range of holding potentials (+75 mV to −75 mV). The individual current amplitudes were clearly greater at negative holding potentials, the unitary conductance increasing from (mean±s.e.mean; $n=6$ patches) 32.41±1.09 pS at +75 mV to 40.4±1.1 pS at −75 mV. Figure 2b shows the *I/V* plot of main state openings from the same patch as in (a); in common with the unitary conductance the mean slope conductance increased from 30 pS at positive potentials to 40 pS at negative potentials. The *I/V* plot for the sub-conductance openings also exhibited inward rectification (Figure 2c); the unitary conductance increased from 26±0.9 pS at +75 mV to 30±1 pS at −75 mV ($n=6$).

Single-channel kinetics

Only the kinetics of the main conductance state of morantel-activated openings were studied (see methods). All the data were obtained from vesicle-attached patches to reduce problems associated with rundown. The resting membrane potential of the vesicle is 0 mV as a result of the displacement of the intravesicular content by the bath solution (Martin *et al.*, 1990) and the single-channel *I/V* relationships of vesicle-attached patches were indistinguishable from those obtained using excised inside-out patches.

Open-times

In general the apparent open-times were best fitted with a single exponential, suggesting the presence of a single open-state for morantel-activated single-channel currents (Table 1). In the presence of low concentrations of morantel (6 nM and 6 μM) the apparent mean open-time was greater at negative holding potentials. For example, with 0.6 μM morantel the mean open-time increased from 0.9 ms at a holding potential of +75 mV to 1.73 ms at −75 mV. These findings suggest that the shutting rate constant, α, is slightly slower at negative than at positive holding potentials. The voltage-sensitivity corresponds to an e-fold increase in the closing rate for every +156 mV change in potential.

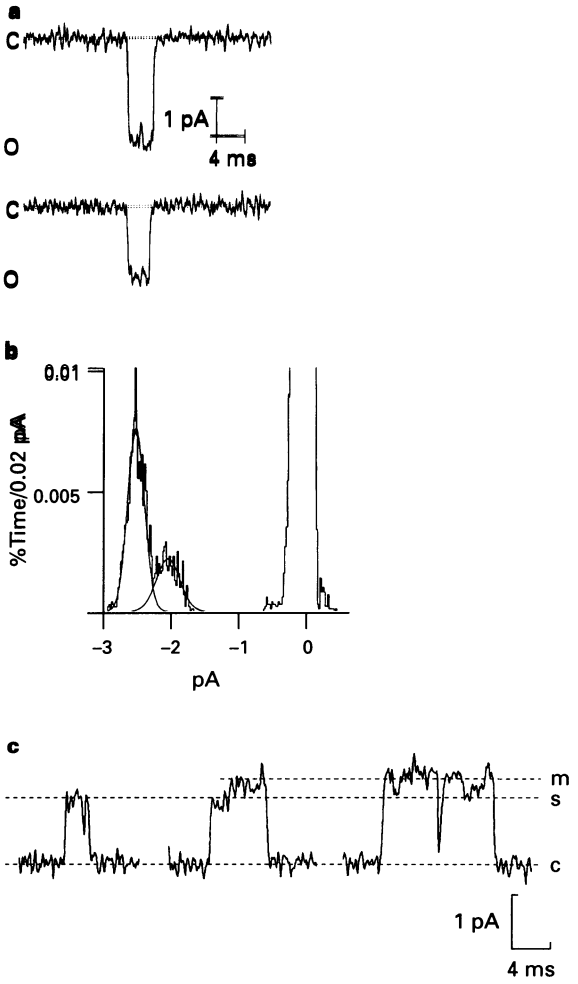

Figure 1 Morantel-activated single-channel currents have at least two conductance states. (a) Examples of the two current amplitudes observed within records of single-channel currents activated by morantel (6 μM) under a holding potential of −50 mV; c, closed-state; o, open-state. In this and all subsequent figures, records of single-channel currents were filtered at 1.5 kHz (-3dB). (b) Patlak amplitude histogram showing the zero current level and the two peaks of the open channel currents. The open channel current was fitted with a double Gaussian giving mean open channel current amplitudes (±s.d.) of 2.0±0.18 pA and 2.5±0.13 pA. The records in (a) and (b) were taken from the same excised inside-out patch under a holding potential of −50 mV. (c) Examples of transitions between the main (m) and sub-conductance (s) states of single-channel currents activated by 6 μM morantel in an excised inside-out patch at a potential of +50 mV. c: closed-state.

Closed-times

Morantel-activated single-channel currents exhibited more complex closed-time distributions. In the absence of channel-block, the closed-time distributions were best fitted by two or three exponential components at both positive and negative holding potentials (Table 2). For example with 6 μM morantel the time constants fitted to the closed-time distribution at +75 mV were 0.13 ms (τ_1), 97 ms (τ_2) and 781 ms (τ_3), reflecting the presence of short, intermediate and long gaps. The short gaps had a duration which was independent of morantel concentration, and were assumed to represent brief closures during single activations of the channel as has been described in previous studies with other agonists (Robertson & Martin,

1993a) and for nicotinic AChRs in muscle and nerve of vertebrates (Colquhoun & Sakmann, 1985). These will be termed 'within-activation' closures. Three time constants were not always resolved because the intermediate component probably represents infrequent events which are too few to allow accurate or consistent identification.

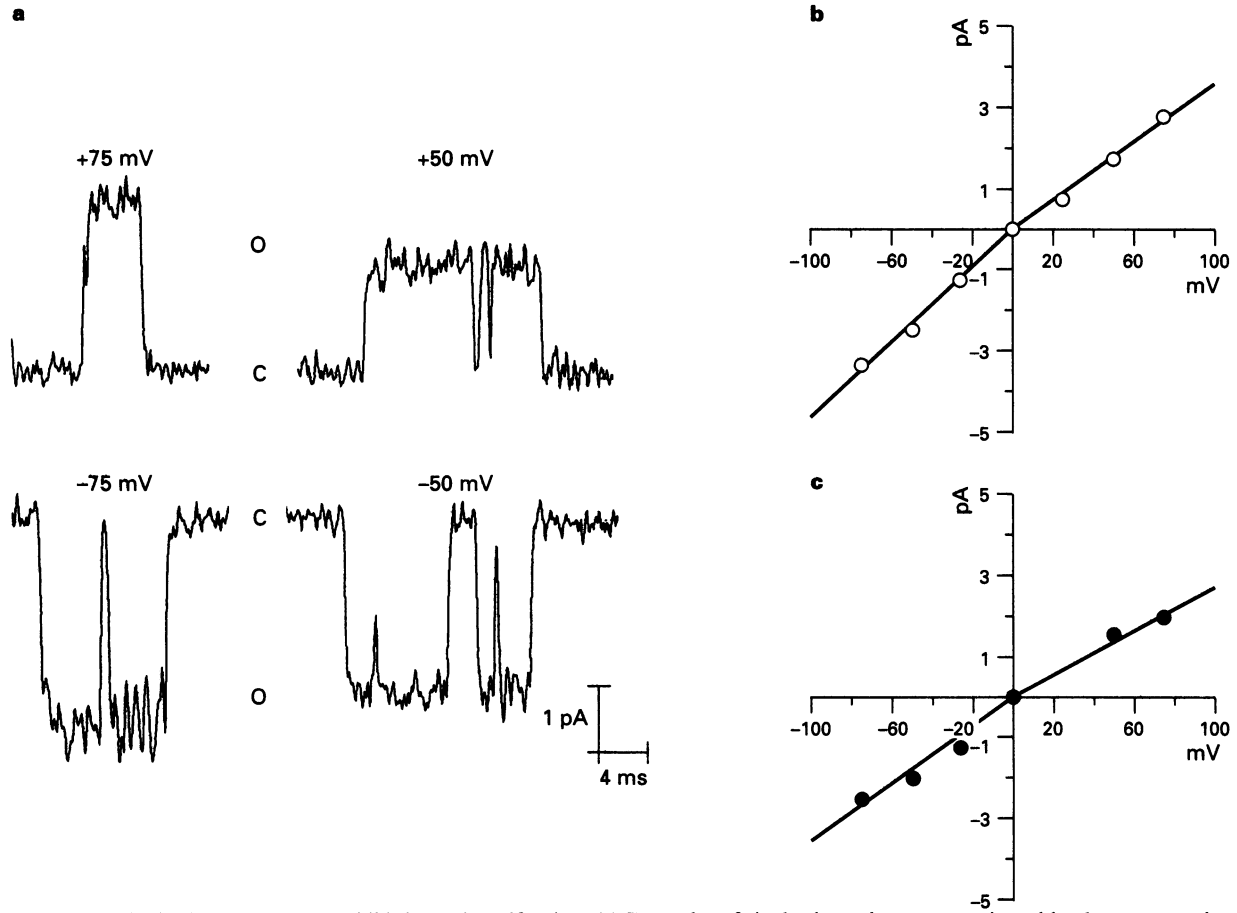

Figure 2 Single channel currents exhibit inward rectification. (a) Examples of single-channel currents activated by 6 μM morantel at four holding potentials (+75 mV, +50 mV, −50 mV and −75 mV), each represents an opening to the main-conductance state. Note the greater amplitude of the currents elicited at negative holding potentials. (b) Current-voltage relationship obtained from the same patch as the records in (a). The data at positive and negative potentials were fitted separately. The cord conductance increased from (mean ± s.e.mean) 30 ± 1.1 pS at positive potentials to 40 ± 1.1 pS at negative potentials, suggesting inward rectification. (c) Current-voltage relationship for openings (not shown) to the sub-conductance state taken from the same patch as (a and b). The unitary conductance was 24 pS at +75 mV and 39 pS at −75 mV. Channels were activated by 6 μM morantel.

Table 1 Open-time kinetics: probability density functions observed at +75 mV and at −75 mV with vesicle attached patches and concentrations of morantel between 0.006 μM and 600 μM

Vm (mV)	*Conc.* (μM)	n	*A1*	*A2*	τ_1 (ms)	τ_2 (ms)
75	0.006	2	1.00	0.00	0.80	
75	0.6	2	1.00	0.00	0.90	
75	6	3	1.00	0.00	0.72 ± 0.07	
75	6	1	0.53	0.47	0.46	1.26
75	10	6	1.00	0.00	0.87 ± 0.10	
75	30	3	1.00	0.00	0.88 ± 0.19	
75	60	3	1.00	0.00	0.81 ± 0.12	
75	100	4	1.00	0.00	0.64 ± 0.13	
75	300	5	1.00	0.00	0.27 ± 0.02	
75	600	6	1.00	0.00	0.25 ± 0.07	
−75	0.006	2	1.00	0.00	1.07	
−75	0.6	2	1.00	0.00	1.73	
−75	6	4	1.00	0.00	1.57 ± 0.24	
−75	10	6	1.00	0.00	1.16 ± 0.11	
−75	30	3	1.00	0.00	0.67 ± 0.15	
−75	60	3	1.00	0.00	0.46 ± 0.05	
−75	100	4	1.00	0.00	0.36 ± 0.04	

Data shown are means ± s.e.mean. In general a single exponential component was distinguished. No single channel events were recorded at 600 μM and too few for analysis at 300 μM morantel at −75mV.

The long time constant was consistently observed and represented a large proportion of the closed-times. Although not studied in detail the duration of the long component was clearly greater with low concentrations (6 nM, $n=2$, Table 2). Taken together with studies relating to mammalian nAChR (Colquhoun & Sackmann, 1985) it is likely that this long component represents the long closures separating individual channel activations and will therefore be termed 'between-activation' closures. As no marked increase in the probability of channel opening (see below), nor decrease in the duration of these long closures was observed between 0.6 μM and 100 μM (Table 2), we were probably close to or beyond the point of saturation of the agonist binding site(s) with 0.6 μM morantel as predicted from the activation by morantel of the macroscopic currents in the somatic muscle cells (Harrow & Gration, 1985). These long 'between-activation' closures may therefore represent an inactive and/or desensitized state of the agonist-receptor complex.

In summary then, at low concentrations the single-channel currents activated by morantel were best described assuming a single open state and two closed states.

Burst-times

At low concentrations (up to 10 μM), at positive and negative potentials, the burst distributions of morantel-activated channels were usually best fitted by one component (Table 3); and the mean burst-time was only slightly greater than the mean open-time of the channels (see Tables 1 and 3). This appeared to be due to the low frequency and brief duration of the 'within-activation' closures (<1 ms; see closed-time kinetics).

At higher morantel concentrations (30 μM – 100 μM), again at positive and negative potentials an additional second longer burst component (Table 3) was separated out and was associated with the appearance of channel-block that is later de-

Table 2 Closed-time kinetics: probability density functions observed at +75 mV and at −75 mV with vesicle attached patches and concentrations of morantel between 0.006 μM and 600 μM

Vm (mV)	*Conc* (μM)	n	*A1*	*A2*	*A3*	*A4*	τ_1 (ms)	τ_2 (ms)	τ_3 (ms)	τ_4 (ms)
75	0.006	2	0.47	0.00	0.53	0.00	0.14		2251	
75	0.6	2	0.07	0.00	0.93	0.00	0.26		949	
75	6	4	0.25±0.18	0.08±0.05	0.67±0.13	0.00	0.13±0.03	97±10	781±575	
75	10	6	0.25±0.18	0.38±0.25	0.37±0.18	0.00	0.44±0.04	148±98	818±294	
75	30	1	0.32	0.68	0.00	0.00	0.19	111		
75	30	2	0.48	0.17	0.35	0.00	0.11	186	836	
75	60	3	0.33±0.04	0.67±0.04	0.00	0.00	0.35±0.01	214.5±47.47		
75	100	4	0.42±0.07	0.25±0.13	0.33±0.16	0.00	0.29±0.04	269±224	835±460	
75	300	5	0.51±0.05	0.10±0.02	0.39±0.03	0.00	0.38±0.02	43.78±15.43	1141±348	
75	600	6	0.55±0.07	0.12±0.04	0.33±0.08	0.00	0.57±0.07	63±0.07	1186±360	
−75	0.006	2	0.22	0.00	0.78	0.00	0.37		2139	
−75	0.6	2	0.44	0.00	0.56	0.00	0.17		1153	
−75	6	4	0.30±0.10	0.21±0.12	0.33±0.02	0.16±0.05	0.49±0.24	12.50±5.00	203±43	940±373
−75	10	6	0.20±0.08	0.33±0.07	0.47±0.07	0.00	0.79±0.39	180±53	978±82	
−75	30	2	0.19	0.00	0.81	0.00	2.39		799	
−75	30	1	0.14	0.23	0.63		1.86	19.12	303	
−75	60	3	0.10±0.02	0.32±0.08	0.58±0.02	0.00	1.96±1.20	72±28	858±193	
−75	100	4	0.00	0.18±0.05	0.40±0.06	0.42±0.07		13.30±5.00	301±133	3376±842

Data shown are means±s.e.mean. Up to four exponential components were distinguished. At −75mV, no single-channel events were recorded at 600 μM and too few were available for analysis at 300 μM morantel.

Table 3 Burst-time kinetics: probability density functions observed at +75 mV and at −75 mV with vesicle attached patches and concentrations of morantel between 0.006 μM and 600 μM

Vm (mV)	*Conc.* (μM)	n	*A1*	*A2*	τ_1 (ms)	τ_2 (ms)
75	0.006	2	1.00	0.00	0.81	
75	0.6	2	1.00	0.00	0.92	
75	6	2	1.00	0.00	0.97	
75	6	2	0.00	0.00	0.46	1.26
75	10	6	0.51	0.49	0.53	1.38
75	30	3	0.00	1.00		1.36±0.26
75	60	3	0.58±0.2	0.42±0.23	0.76±0.24	3.5±1.8
75	100	4	0.52±0.1	0.48±0.16	0.69±0.32	2.66±0.62
75	300	5	0.00	1.00		1.14±0.21
75	600	6	0.00	1.00		1.09±1.15
−75	0.006	2	1.00	0.00	1.9	
−75	0.6	2	1.00	0.00	2.01	
−75	6	4	1.00	0.00	2.41±0.36	
−75	10	6	1.00	0.00	1.73±0.21	
−75	30	1	1.00	0.00	1.39	
−75	30	2	0.71	0.29	0.58	5.74
−75	60	3	0.83±0.0	0.19±0.01	0.46±0.01	2.78±1.34
−75	100	4	0.83±0.0	0.17±0.02	0.43±0.06	12.39±5.84

Data shown are means±s.e.mean. Up to two exponential components were required to describe the burst distributions. At −75 mV, no single-channel events were recorded at 600 μM and too few events were observed for analysis at 300 μM morantel.

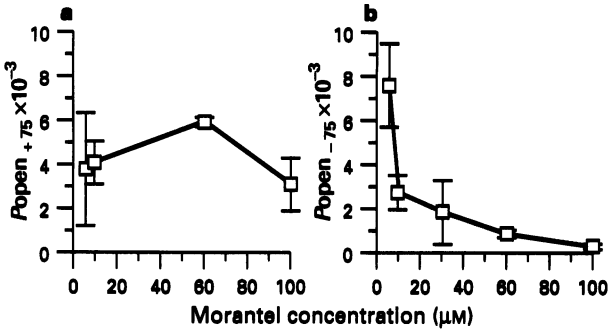

Figure 3 A concentration-dependent decline in *Po* is observed at negative but not positive holding potentials. Plots of the probability of channel opening against morantel concentration at (a) +75 mV and (b) −75 mV. Each point represents the mean of at least three observations from patches where the activity of only a single channel was evident. The vertical bars represent the s.e.mean of each set of data.

scribed in detail. The brief burst-time constant, τ_1, then described 'short bursts' that had similar durations to mean open-times. The longer burst-time constant, τ_2, described 'long bursts' that were due to sequences of openings separated by short 'within-activation' closures and/or short block periods.

Increasing morantel concentration decreases Po *at negative but not positive potentials*

At positive potentials the probability of channel opening (*Po*) appeared constant and independent of morantel concentration between 6 μM ($3.83 \pm 2.6 \times 10^{-3}$; mean ± s.e.mean, $n = 4$) and 100 μM (3.19 ± 10^{-3}; $n = 4$), suggesting that we were at or approaching saturation of the nicotinic AChR agonist binding site(s) as predicted from the studies of the macroscopic currents activated by morantel (Harrow & Gration, 1985). This point is illustrated in Figure 3a, which shows a plot of *Po* against morantel concentration at a holding potential of +75 mV. Between 100 μM and 600 μM morantel, however, a small concentration-dependent reduction in *Po* was observed (not shown) associated with the onset of a fast-flickering open channel-block.

At negative holding potentials a marked concentration-dependent reduction in *Po* was observed between 6 μM and 100 μM morantel. This is illustrated in Figure 3b which shows a plot of *Po* against morantel concentration, obtained with a holding potential of −75 mV; *Po* declined from $7.68 \pm 1.89 \times 10^{-3}$ ($n = 4$) at 6 μM to $0.31 \pm 0.12 \times 10^{-3}$ ($n = 4$) at 100 μM. The decline in *Po* resulted from the complex form of open channel-block that is considered subsequently.

A flickering channel-block occurs at positive potentials

A fast-flickering open channel-block was observed at positive holding potentials as the concentration of morantel was increased over the range 100 μM to 600 μM. Figure 4a shows the fast-flickering channel-block with channel openings recorded in the presence of 600 μM morantel over a range of positive holding potentials (+125 mV to +50 mV). It can be seen that the duration and frequency of the block events increases as the holding potential was made less positive, an effect consistent with the cationic nature of morantel. This channel-block led to a concentration-dependent reduction in the mean open-time

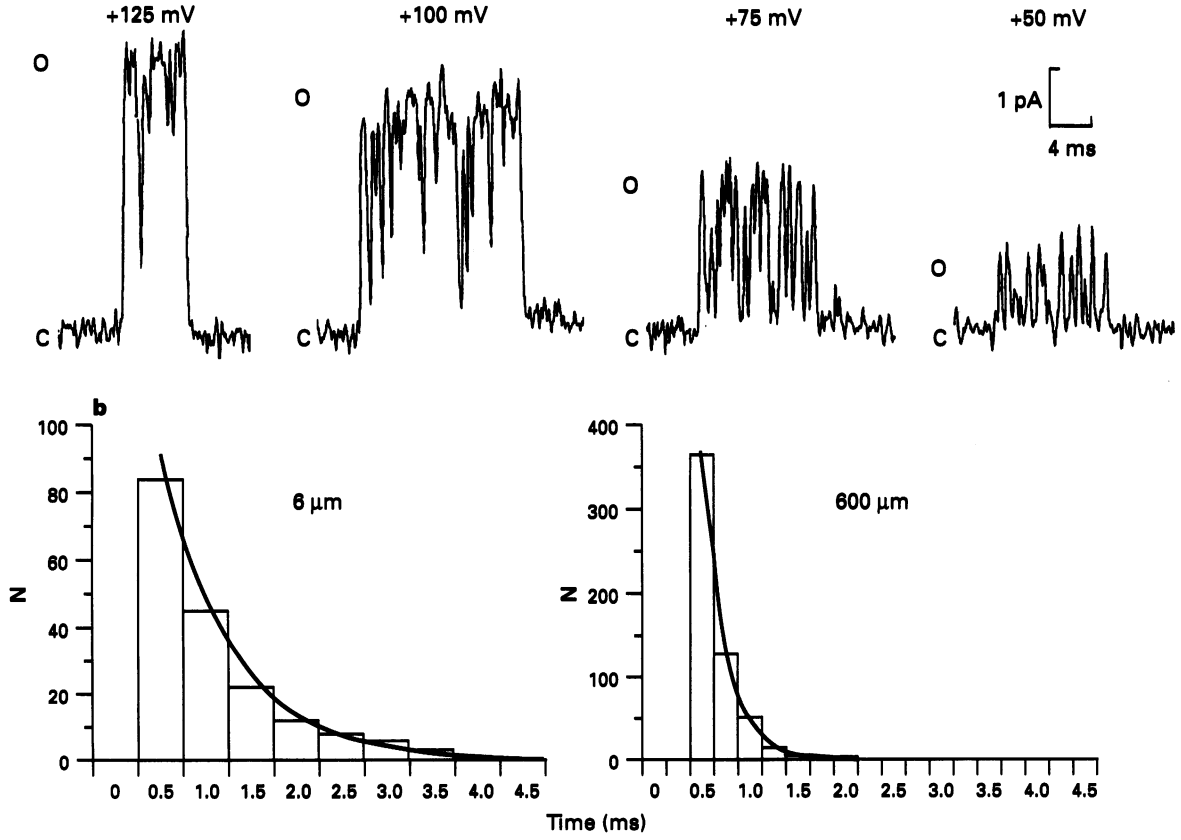

Figure 4 With high concentration of morantel fast flickering open channel-block is observed at positive potentials. (a) Fast flickering block of single-channel currents activated by 600 μM morantel at +125 mV, +100 mV, +75 mV and +50 mV; vesicle-attached patch configuration. Note the increase in the frequency and duration of the block as the holding potential is made less positive (+125 mV to +50 mV). Records were obtained in the vesicle-attached patch configuration. c, closed; o, open. (b) Open-time distributions. Single exponential fits to open-time histograms obtained in the presence of 6 and 600 μM morantel and a pipette potential of +75 mV; the time constants fitted were 0.8 ms and 0.25 ms respectively. N is the number of channel openings.

from 0.72 ± 0.07 ms (mean $\pm$ s.e.) with 6 μM morantel to 0.25 ± 0.7 ms with 600 μM morantel, Figure 4b and Table 1.

Fast-flickering channel-block has been explained by a simple open channel-block mechanism (Adams, 1976; Neher & Steinbach, 1978) in which a single large-blocking-ion moves repeatedly into and out of the open ion-channel. In the following sections we describe properties of the channel-block at positive potentials and show that it has properties inconsistent with the simple channel-block mechanism.

The channel-blocking rate, k_{+B}, at positive potentials Figure 5a illustrates plots of reciprocal mean open-time against morantel concentration for holding potentials of +100 mV, +75 mV and +50 mV. It is likely that the gradients of such plots are a valid method of estimating the channel-blocking rate, k_{+B}, for a variety of complicated processes governing channel-block (Ogden & Colquhoun, 1985). For each plot the line was fitted by the method of least squares; the slope ($\pm$s.e.mean) gave values for k_{+B} of $3.3 \pm 0.9 \times 10^6$ M^{-1} s^{-1}, $6.1 \pm 1.4 \times 10^6$ M^{-1} s^{-1} and $9.8 \pm 0.7 \times 10^6$ M^{-1} s^{-1} at +100 mV, +75 mV and +50 mV, respectively. Clearly then k_{+B} increased as the holding potential was made less positive.

k_{+B} is also a factor determining the slope of blockage frequency plots, but the slopes of these plots are proportionately less than k_{+B} if simple channel-block does not occur and if the blocked state can enter other closed or blocked states without directly reopening (Ogden & Colquhoun, 1985). Figure 5b shows plots of the number of block durations per unit open-time against morantel concentration, the slopes of which had values of 2.3×10^6 $M^{-1}s^{-1}$ at +75 mV and 5.8×10^6 $M^{-1}s^{-1}$ at +50 mV. These slopes are similar but less than the previously estimated k_{+B} values suggesting that the blocked state is able to enter another closed or blocked state without always having to reopen.

Voltage-sensitivity of k_{+B} at positive potentials Figure 6a describes the voltage-sensitivity of k_{+B} (obtained from plots of 1/mean open-time) against the positive holding potential with a line fitted by the method of least squares to the observations. The slope of the line, V_K, predicts an e-fold decrease in k_{+B} for every +46 mV change in membrane potential and the intercept predicts that k_{+B} at 0 mV has a value of 2.94×10^7 $M^{-1}s^{-1}$.

The voltage-dependence of ion channel-blocking rates has been explained by a Woodhull model (Neher & Steinbach 1978; Hille 1992) and the relative position of the block site within the channel determined from the voltage-sensitivity. δ, the relative or apparent electrical distance from the extracellular surface of the pore is $2(F/RT)/k_{+B}$, where F, R and T have their usual meaning and for our purposes F/RT is 25 mV at 20°C. From our data we obtain a relative electrical distance (δ) of 1.1, greater than the width of the channel: this value cannot be explained by a single block site within the channel. One explanation, considered later, for the large and apparently impossible δ may be that of multi-ion channel-block (Hille, 1992).

The block duration at positive potentials and its voltage-sensitivity

The channel unblocking rate, k_{-B}, would be equal to the reciprocal of the mean block duration if the fast-flickering block were governed by a simple open channel-block mechanism

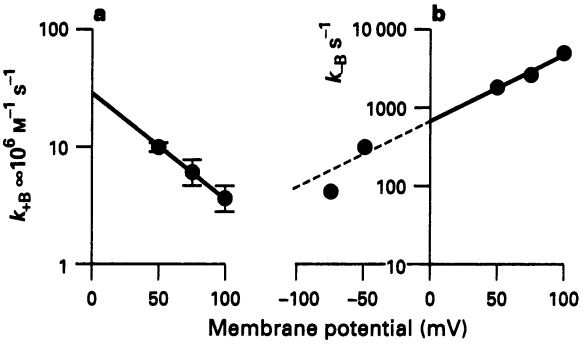

Figure 6 The forward blocking and unblocking rate constants are voltage-sensitive. (a) k_{+B} versus membrane potential; (b) k_{-B} versus membrane potential. The lines were fitted by least squares. From the intercept of each line on the abscissa scale values of 2.94×10^7 $M^{-1}s^{-1}$ and $765\,s^{-1}$ were obtained for k_{+B} and k_{-B}, respectively, at 0 mV. The slopes predict an e-fold decrease in k_{+B} for every +46 mV change in potential and an e-fold increase in k_{-B} for +44 mV change in holding potential. The vertical bars represent s.e.mean of each set of data.

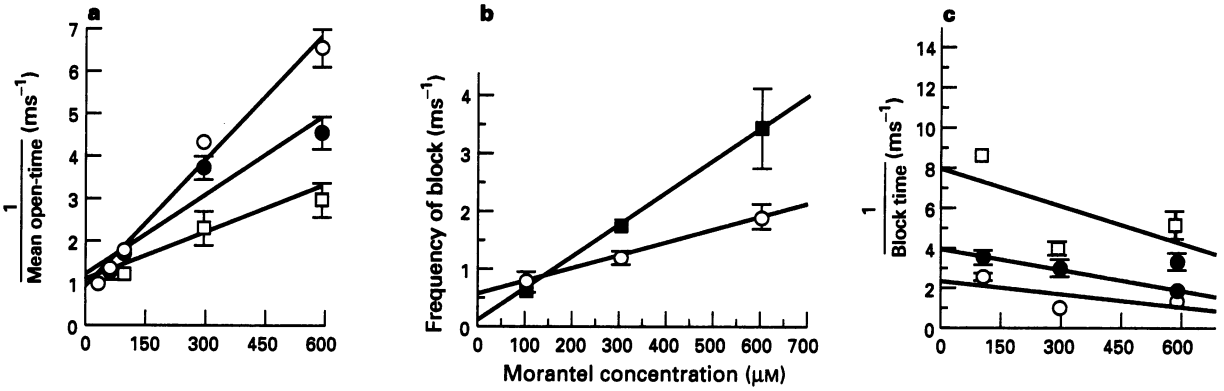

Figure 5 Estimation of the forward blocking and unblocking rate constants. (a) Plot of the reciprocal mean open-time against morantel concentration for holding potentials of +100 mV (□) +75 mV (○) and +50 mV (●). Lines were fitted to the points by least squares. The slope of the lines predicted values ($\pm$s.e.mean) for the forward blocking rate constant, k_{+B}, at $3.37 \pm 0.88 \times 10^6 M^{-1}s^{-1}$ (+100 mV), $6.14 \pm 1.36 \times 10^6 M^{-1}s^{-1}$ (+75 mV) and $9.84 \pm 0.74 \times 10^6 M^{-1}s^{-1}$ (+50 mV). Intercepts with the abscissa scale predicted values of $104.1\,s^{-1}$ (+100 mV), $1185\,s^{-1}$ (+75 mV) and $891\,s^{-1}$ (+50 mV) for the channel closing rate constant α. (b) Plot of the frequency of block against morantel concentration under holding potentials of +75 mV (○) and +50 mV (■). Estimates of the frequency of block were obtained by dividing the total open-time by the estimated total number of short gaps. Each point represents the mean of at least three observations. The slope of the plot was $6 \times 10^6 M^{-1}s^{-1}$ at +50 mV and $3 \times 10^6 M^{-1}s^{-1}$ at +75 mV. (c) The reciprocal of the duration of the short block against morantel concentration for patch potentials of +100 mV (□) +75 mV (○) and +50 mV (●). The correlation between reciprocal block time and morantel concentration was not significant. The points represent the mean of at least three observations. In all sections the vertical bars represent s.e.mean of each set of data.

(Adams, 1976; Neher & Steinbach, 1978) or, in more complex schemes, as we suspect here, be equal to the sum of all exit rates from the blocked state. The reciprocal of the mean block duration then provides an upper estimate for k_{-B}.

Figure 5c shows a plot of the reciprocal of the block duration against morantel concentration for a holding potential of +100 mV, +75 mV and +50 mV. There was no significant correlation between morantel concentration and the mean block durations at any of the holding potentials studied. As might be expected for the cation morantel, the block duration decreased as the holding potential was made more positive, giving upper limits for k_{-B} at +100 mV (100–600 μM), +75 mV (100–600 μM) and +50 mV (100 μM–600 μM) in the region of (mean ± s.e.mean) 5165 ± 746 s^{-1}, 2781 ± 254 s^{-1} and 1878 ± 226 s^{-1}, respectively.

Figure 6b shows a semi-log plot of the upper estimates for k_{-B} against potential and the line fitted to the points observed at positive potentials by the method of least squares. We find the intercept with the abscissa at 0 mV to be 767 s^{-1}, while the slope, V_k, shows an e-fold decrease every −44 mV change in membrane potential, which is numerically close to but opposite in polarity to the voltage-sensitivity of the blocking rate, k_{+B}. Although the interpretation of the voltage-sensitivity of these estimated blocking rates for k_{+B}, depends on the blocking mechanism involved we can again say that observations do not support a simple channel-block mechanism because the predicted relative electrical distance of the site of block would be 1.1 and greater than the width of the channel.

The flickering-block at positive potentials then shows a number of features not consistent with the simple block. In addition, Table 3 shows at positive potentials, that the mean duration (t_2) of the 'long bursts', did not increase linearly with concentration in the range 30 μM–100 μM in a manner predicted by the simple open channel-block mechanism. Further inconsistencies were seen at negative potentials.

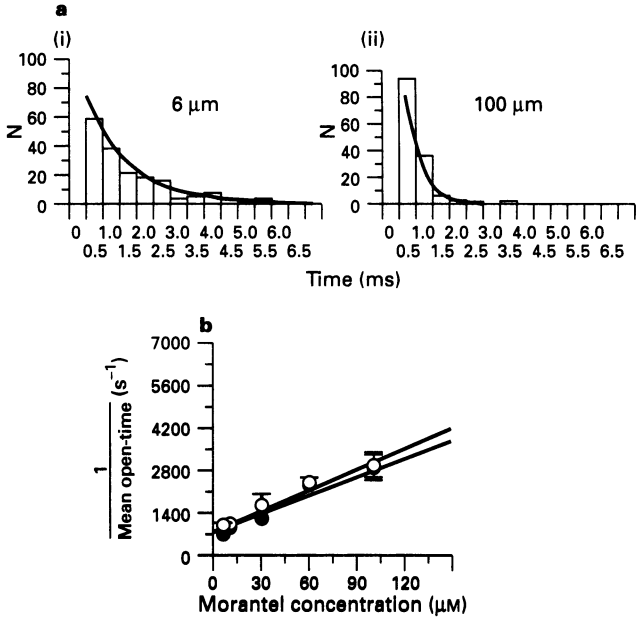

Figure 7 Concentration-dependent reduction in mean open-time at negative holding potentials. (a) Single exponential fits to open-time distributions obtained in the presence of (i) 6 and (ii) 100 μM morantel and a pipette potential of −75 mV; the time constants fitted were 1.28 ms (6 μM) and 0.43 ms (100 μM). N is the number of channel openings. (b) Plots of the reciprocal of mean open-time against morantel concentration for holding potentials of −50 mV (●) and −75 mV (○). The lines were fitted by least squares. The slope had a value of $2.27 \pm 0.3 \times 10\,M^{-1}s^{-1}$ at −50 mV and $1.9 \pm 0.3 \times 10^7\,M^{-1}s^{-1}$ at −75 mV. The intercept of the lines was 773 s^{-1} at −50 mV and 745 s^{-1} at −75 mV.

Channel-block and open- and closed-times at negative potentials

We have commented earlier on the marked concentration-dependent reduction in *Po* observed with negative holding potentials. The mechanism underlying this decline in *Po* involved effects on open-times and on closed-times.

Effect on open-times At negative potentials a concentration-dependent reduction in mean open-time occurred between 6 μM and 100 μM morantel (Table 1). Figure 7a shows examples of the open-time distributions obtained at 6 μM and 100 μM. The time constants fitted declined from 1.57 ms with 6 μM to 0.36 ms with 100 μM morantel (Table 1). The slope of the relationship between the reciprocal of the mean open-time and morantel concentration was linear and is a measure of the channel blocking rate, k_{+B}. Figure 7b shows such plots for holding potentials of −50 mV and −75 mV, each line was fitted by the method of least squares. The slope for the two potentials was nearly the same: $2.3 \times 10^7\,M^{-1}s^{-1}$ at −50 mV and $1.9 \times 10^7\,M^{-1}s^{-1}$ at −75 mV.

The values of k_{+B} at −50 mV and −75 mV are almost identical to that of k_{+B0} estimated from the analysis of the flickering channel-block observed at positive potentials: $2 \times 10^7\,M^{-1}s^{-1}$ (Figure 6a). This may be explained if a potential barrier acts as the rate limiting step for k_{+B} at positive potentials but a voltage-insensitive diffusion-barrier becomes the rate-limiting step for k_{+B} at negative membrane potentials. However, the reduction in mean open-time does not explain the marked concentration- and potential-dependent decline in *Po* measured under negative holding potentials, particularly when we consider the loss of voltage-sensitivity of k_{+B} at negative potentials.

Effect on closed-times At negative holding potentials a concentration- and voltage-dependent increase in mean closed-time was observed. At −75 mV the mean closed-time increased from (mean ± s.e.mean) 224 ± 42 at 6 μM to 1908 ± 506 at 100 μM and the changes in the closed-time distributions resulted in the appearance of two distinctive voltage-sensitive gap components: a 'short block' and a 'long block'.

Short block One of these gap components was short (mean duration ~13 ms) and is referred to here as the short block. The short block had a duration that appeared independent of morantel concentration. It was first noticed at low frequencies with 6 μM morantel at −75 mV when the best fit to the closed-time distribution increased from three to four exponential components; under these conditions the short block had a duration of 12.5 ms ($t2$; Table 2). Between 6 μM and 100 μM, the short block was not resolved due to aggregation with 'within-activation' channel closures. However, in the presence of 100 μM morantel the channel openings occurred singly or in doublets (Figure 8b) separated by gaps with a mean duration of 13.3 ms (Table 2, $t1$, 100 μM −75 mV). Under these conditions the short block represented the majority of the short gaps observed; few if any brief 'within-activation' closures were observed.

Although the duration of the short block was not concentration-dependent, it was voltage-dependent (Figure 9d, Table 2) and was related to the block periods measured at positive holding potentials. When the line fitted to the relationship between the reciprocal of the block time (k_{-B}) and holding potential at positive potentials was extrapolated to −50 mV and −75 mV, it accurately predicted the duration of the short gaps observed at both negative potentials when 100 μM morantel was present (Figure 6c) suggesting that its origin was the same.

Long block The other gap component was long (seconds), increased in duration with concentration, and is referred to here as the long block. The concentration-dependent nature of the long block is illustrated in Figure 8c which compares ty-

pical single channel records obtained at +75 mV and −75 mV in the presence of 10, 100 and 600 μM morantel. The long block observed at −75 mV with 100 μM morantel increased in duration still further when the concentration was raised to 600 μM, such that open events were not observed in records as long as 10 min. These long block gaps were absent at positive potentials and their appearance showed no time-dependence: they were observed at negative potentials immediately after patch formation and disappeared when the holding potential was made positive (+50, +75 or +100 mV).

Figure 9a shows representative closed-time distributions obtained in the presence of 0.6 μM morantel at +75 mV and −75 mV: there is no real difference in the duration of the long time constants fitted at the two potentials. Figures 9b, c and d show representative closed-time distributions obtained with 30, 60 and 100 μM morantel at +75 mV and −75 mV: at −75 mV a concentration- and voltage-dependent increase in the longest gap component is observed; the mean duration of the longest time constant fitted to the closed-time distribution at −75 mV with 30 μM morantel concentration was 303 ms, with 60 μM it was 990 ms, and with 100 μM it was 4016 ms. Figure 9d shows that a clear separation was obtained at 100 μM morantel between the long block and the 'between-activation' closures: 'between-activation' closures were identified by the fact that their mean duration remained virtually the same at +75 mV (813 ms) and −75 mV (517 ms). It is pointed out, however, that the simple averages of closed-time constants (Table 2) observed in different preparations only indicate the presence of the concentration- and voltage-dependent long block when concentrations at 60 μM or greater are used and the longest gap component at +75 mV is compared with the longest gap component at −75 mV. Variability between patch recordings associated with the heterogeneous population of channels and animals (see Martin *et al.*, 1991) may have lead to aggregation of the long block with 'between-activation' closures at lower concentrations.

Degree of block shows cooperativity

The degree of block may be defined as Po_{-75}/Po_{+75} providing the following assumptions are valid: (1) In the absence of channel-block there is no significant increase in *Po* with morantel concentration over the range 0.6–100 μM. This seems valid from the relationship between *Po* and concentration measured under a holding potential of +75 mV (Figure 3a).

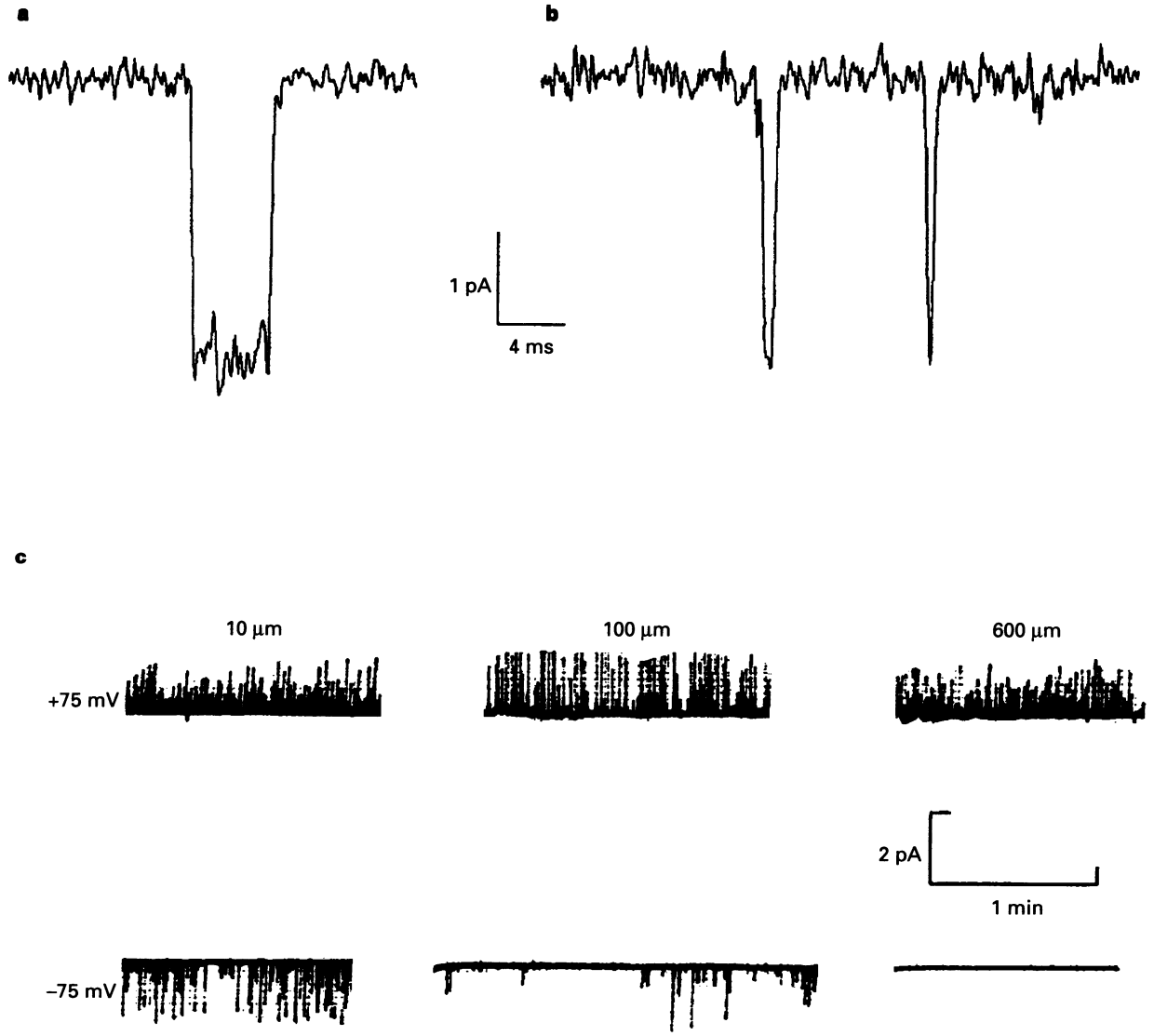

Figure 8 The short block and concentration-dependent long block gaps at negative holding potentials. (a) Typical opening produced by 6 μM morantel; note the single uninterrupted opening lasting 4 ms, −75 mV. (b) A 'doublet' of brief openings separated by the short block observed in the presence of 100 μM morantel, −75 mV. (c) Concentration- and voltage-dependence of the additional long block gap observed in the presence of morantel is illustrated at lower time resolution; current records were activated by 10 μM, 100 μM and 600 μM morantel recorded at +75 mV and −75 mV. Recordings were made in the vesicle-attached patch configuration, first at −75 mV and then at +75 mV.

(2) Between 0.6 μM and 100 μM, the reduction in Po resulting from channel-block at +75 mV is small relative to the reduction in Po observed at negative holding potentials, and may be ignored. (3) In the absence of channel-block the ratio Po_{-75}/Po_{+75} would be constant and independent of morantel concentration. Figure 10a shows a plot of Po_{-75}/Po_{+75} against

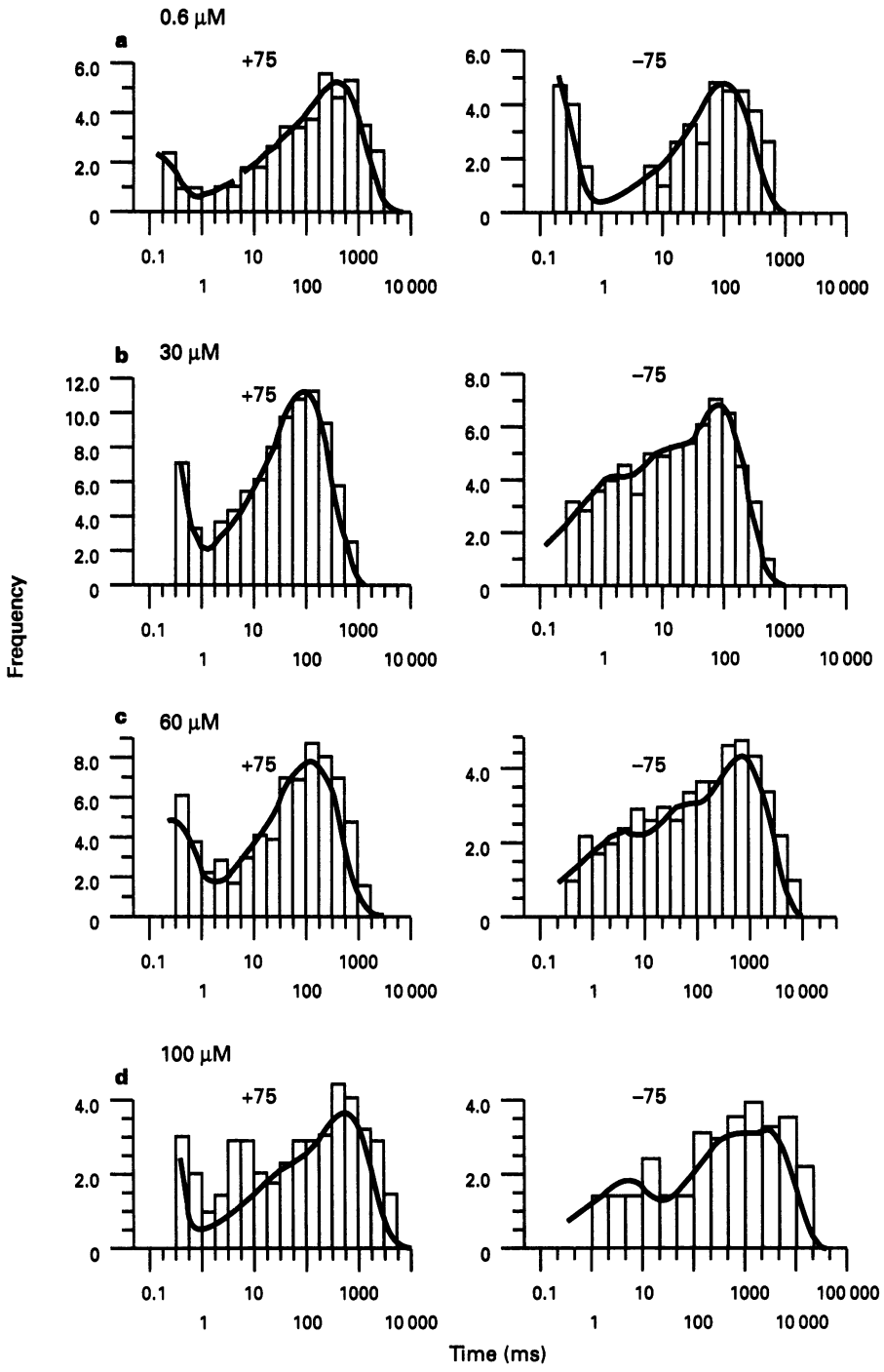

Figure 9 Concentration- and voltage-dependence of the longest gap component in the closed-time distributions. Distributions of closed-times obtained in the presence of different concentrations of morantel at +75 mV and −75 mV are shown on a log scale (abscissa scales 4 bins per log unit except for (d) −75 where 3 bins per log unit was used) against the square root of frequencies (ordinate scales) and maximum likelihood fits to each individual closed time (see methods pdfs) shown by continuous lines. In (a–d) distributions at −75 mV (right panels) were obtained immediately after patch formation and then distributions at +75 mV (left panels) were obtained subsequently from the same patch. (a) +75: Distributions obtained with 0.6 μM morantel, +75 mV, three exponentials fitted, $\tau_1 = 0.12$ ms (area 0.16), $\tau_2 = 38.5$ ms (area 0.08) and $\tau_3 = 510$ ms (area 0.76). (a) −75: The duration of the longest time constant fitted was similar when the holding potential was −75 mV; two exponentials fitted, $\tau_1 = 0.17$ ms (area 0.50) and $\tau_2 = 570$ ms (area 0.50). (b) +75: Distributions obtained with 30 μM morantel, +75 mV, two exponentials fitted, $\tau_1 = 0.19$ ms (area 0.32) and $\tau_2 = 111$ ms (area 0.68). (b) −75: At −75 mV the duration of the longest time constant was greater, $\tau_1 = 1.9$ ms (area 0.14), $\tau_2 = 19$ ms (area 0.20) and $\tau_3 = 303$ ms (area 0.66). (c) +75: Distributions obtained with 60 μM morantel, +75 mV, two exponentials fitted, $\tau_1 = 0.27$ ms (area 0.26) and $\tau_2 = 187$ ms (area 0.74). (c) −75: At −75 mV the duration of the longest time constant is much longer; $\tau_1 = 3.9$ ms (area 0.13), $\tau_2 = 55$ ms (area 0.21) and $\tau_3 = 990$ ms (area 0.66). (d) +75: 100 μM morantel, +75 mV, three exponentials fitted, $\tau_1 = 0.13$ ms (area 0.73), $\tau_2 = 50$ ms (area 0.045) and $\tau_3 = 813$ ms (area 0.225). (d) −75: At −75 mV the longest time constant (long block gaps) exceeded those observed with 30 μM or 60 μM morantel, $\tau_1 = 7$ ms (area 0.16), $\tau_2 = 517$ ms (area 0.30) and $\tau_3 = 4016$ ms (area 0.54).

morantel concentration. The relationship was fitted by non-linear least squares regression to the Hill equation:

$$R = \frac{R_{max}}{1 + (\frac{x_a}{IC_{50}})^{n_H}}$$

where R represents the degree of block at concentrations x_a, IC_{50} the concentration at which 50% block was observed and n_H the Hill coefficient. R_{max} is the ratio Po_{-75}/Po_{+75} in the absence of block. The best fit was obtained with an R_{max} of 2.9, IC_{50} of 10 μM and n_H of 1.6. A value for n_H greater than 1 suggests the involvement of at least two blocking molecules.

The use of the ratio Po_{-75}/Po_{+75} has the advantage of being able to normalize the data and so reducing inter-patch variability. We also fitted the Hill equation to the plot of Po_{-75} against morantel concentrations >than 0.6 μM (Figure 10b) and found that it had a similar n_H value (1.7), suggesting that our ratio analysis is not compromised.

Sequential double block model

In order to describe the positive cooperativity shown by the block quantitatively, we have used a minimal model describing a two-ion open channel-block (Evans & Martin, 1992b; Evans & Martin, 1993a,b). The simple channel-block model was extended to incorporate a second binding site for morantel within the channel pore:

$$\boxed{C} \underset{\beta'}{\overset{\alpha}{\rightleftharpoons}} O \underset{k_{-B'}}{\overset{k_{+B'}.x_a}{\rightleftharpoons}} MB1 \underset{\delta}{\overset{\gamma}{\rightleftharpoons}} MB2 \underset{k_{-B'}}{\overset{k_{+B'}.x_a}{\rightleftharpoons}} MB1MB2$$

where $\boxed{C}$ is the distinguishable closed state and O is open, MB1 represents the occupation of a block site near the mouth of the pore, MB2 represents the occupation of a second block site deeper within the pore, and MB1MB2 represents a double occupation. $\beta'\alpha$, k_{+B}, k_{-B}, γ, δ, $k_{+B'}$ are rate constants and x_a represents the morantel concentration.

The model requires that: the occupation of the site MB1 by a molecule of morantel allows access, by that molecule alone, to site MB2; it allows MB1 to be occupied while MB2 is occupied; but does not allow a molecule bound to MB2 to leave the channel pore while MB1 is occupied. Thus as the concentration of morantel is increased the frequency of occupation of MB1 and thus MB2 increases; furthermore, the frequency of double occupation and thus the duration of time the molecule bound to site MB2 is held within the pore also increases. Hence the model may explain the occurrence of the additional long gaps with a duration dependent on morantel concentration.

The model is simplified with only one closed-state opening: we excluded the brief 'within-activation' closed-state from the model as it does not influence greatly the *Po*-morantel-concentration relationship. Also, we have ignored the concentration-dependence of the opening rate constant β' as we appeared to be at or beyond the point of receptor saturation with the lowest concentrations studied.

The relationship between the degree of block and morantel concentration predicted by this model may be determined from the principles of microscopic reversibility. The model describing the double-ion block of the channel pore predicts that if there is little or no block at +75 mV and we let

$R = (1 + \frac{\alpha_{+75}}{\beta'_{+75}})/(1 + \frac{\alpha_{-75}}{\beta'_{-75}})$ then :

$$\frac{P_{o-75}}{P_{o+75}} = \frac{R}{1 + \frac{\beta'}{\alpha+\beta'}(\frac{x_a}{K_B} + \frac{x_a}{K_B}\cdot\frac{\gamma}{\delta} + \frac{\gamma}{\delta}\cdot\frac{x_a^2}{K_B.K'_B})} \qquad (2)$$

Where $\beta'/(\alpha+\beta')$ are the values at −75 mV; K_B is k_{-B}/k_{+B} at −75 mV; K'_B is k'_{-B}/k'_{+B} at −75 mV and γ/δ are also at −75 mV.

Estimation of some of the parameters of equation 2 We can already provide estimates for a number of the parameters described in equation 2 from our experimental records. R was taken as 2.71, the ratio Po_{-75}/Po_{+75} in the presence of 0.6 μM morantel when little or no block was observed at −75 mV. This is nearly the same as R_{max} estimated from the fit to the Hill equation (Figure 10a). $\beta'/(\alpha+\beta')$ was taken as *Po* in the presence of 0.6 μM morantel at a holding potential of −75 mV, when little or no block was observed: this was 0.004.

For the proposed sequential double block scheme, a plot of the reciprocal of mean open-time against morantel concentration would have an intercept of $1/\alpha$ and a slope of k_{+B}. As we showed earlier this plot gave a value for k_{+B} of 1.9×10^7 $M^{-1}s^{-1}$ at −75 mV (Figure 7b). If, as we suspect, MB1 represents the same binding site as that conferring block at positive potentials, then k_{+B} loses its voltage-sensitivity at negative holding potentials.

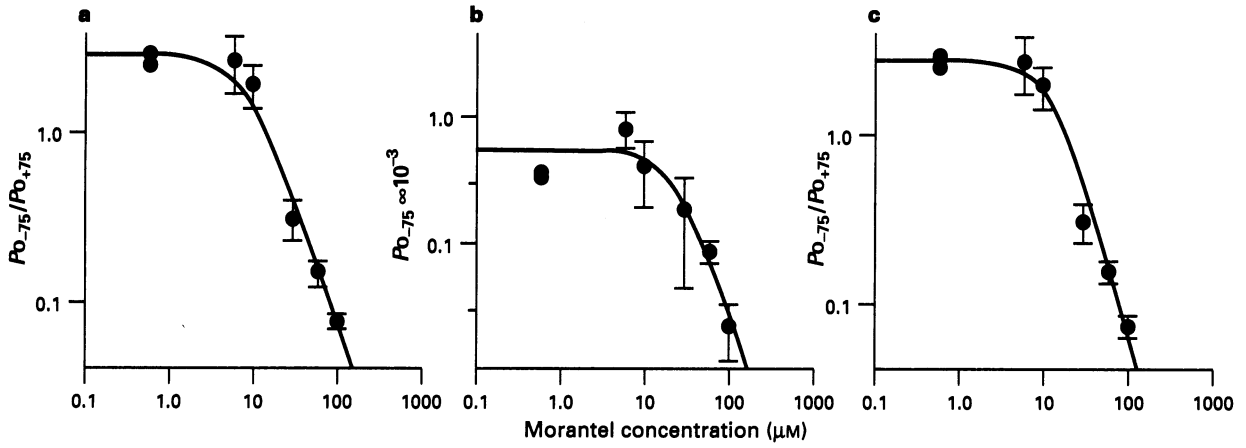

Figure 10 The relationship between *Po* and morantel concentration suggests positive cooperativity between at least two blocking molecules. (a), (b) and (c) show log-log plots of the degree of block against morantel concentration. The vertical bars represent s.e.mean for each set of data which comprise at least three observations. (a) Po_{-75}/Po_{+75} is plotted against morantel concentration, with the line representing the least squares fit to the Hill equation which gave values of 10 μM for the IC_{50} and 1.6 for n_H. This suggests positive cooperativity between at least two blocking molecules. (b) The Hill plot of Po_{-75} against morantel concentrations greater than 0.6 μM (12 μM for the IC_{50} and 1.7 for n_H). (c) The same data as in (a) fitted by least squares to equation 2, the limiting slope was close to 1.6, as for (a) and (b).

The sequential model also predicts that at a given holding potential, the sum of the rate constants, k_{-B} and γ, may be derived from the reciprocal of the mean duration of the short block periods (τ_1 or 13.3 ms; Table 2) in the presence of 100 μM morantel and a holding potential of -75 mV. At this point the degree of block is high and we may assume that the majority of the short gaps represent the short block periods and few if any short 'within-activation closures' occur.

Estimation of remaining parameters of equation 2 by non-linear regression

The values of the parameters mentioned above (k_{+B},$k_{-B}+\gamma$, R and $\beta'/(\alpha+\beta')$) were fixed and the remaining parameters of equation 2 determined from non-linear least squares fits to the relationship between Po_{-75}/Po_{+75} and morantel concentration. We found that it was possible to make estimates of the three parameters: K_B, K'_B and γ/δ, if the estimates for K'_B were constrained in the analysis to be equal or greater than K_B. This is reasonable since prior entry of one molecule of morantel into the channel and binding at MB2 might slow the entry rate (k'_{+B}) of a second molecule by repulsion as well as increasing its exit rate (k'_{-B}). Fixing these parameters then allowed estimation of the following rate constants: k_{+B}, 2×10^7 $M^{-1}s^{-1}$; k_{-B}, 22.01 s^{-1}, γ, 54 s^{-1}; δ, 54 s^{-1}. K_B and K'_B were found to have the same value, 1.1 μM, suggesting that the dissociation constant at the first block site does not increase when the second block site MB2 is occupied. Figure 10c shows the line of best fit obtained for equation 2, with the parameters above, and that the limiting slope of the plot was near at 1.6. The plot shows that equation 2, and thus the sequential model, describes our experimental observations. In contrast, the simple channel-block scheme (Adams, 1976; Neher & Steinbach, 1978) and a simple sequential model, where the blocked state enters a single desensitized state, failed to describe our experimental data.

Morantel does not block nicotinic AChR currents when applied to the cytoplasmic surface of the patch

When single nitotinic AChRs were activated in excised inside-out patches by addition of 0.6 μM morantel to the pipette solution, a concentration with which no channel-block was observed, bath application of 1 mM morantel to the cytoplasmic surface of the patch altered neither the single-channel conductance, mean open-time nor Po (not shown). These findings are similar to the effects observed at the *Ascaris* nicotinic AChR with levamisole (Robertson & Martin, 1993b).

Discussion

Conductance properties

The nicotinic-acetylcholine receptors (AChR) from the somatic muscle cells of *Ascaris* displayed at least two conductance states when activated by morantel as has been observed for acetylcholine- and levamisole-activated single-channel currents (Pennington & Martin, 1990; Robertson & Martin, 1993a). Both main- and sub-conductance states exhibited inward rectification. The main-conductance increased from a mean of 32 pS at +75 mV to 40 pS at -75 mV. Although the inward rectification has not been obtained in the *Ascaris* preparation previously, such rectification has been seen in studies of rat sympathetic ganglionic nicotinic AChRs (Mathie *et al.*, 1990) and Torpedo nicotinic AChRs (Imoto *et al.*, 1988). As for these nicotinic AChRs our results in *Ascaris* may be explained by an asymmetrical organization of the pore of the *Ascaris* channel, which is suggested by the fact that the block produced by morantel and another agonist levamisole (Robertson & Martin, 1993b) only occurred when the drug was present at the extracellular but not cytoplasmic surface of the patches. With a symmetrical pore one would expect to observe block after application to extracellular and intracellular surfaces.

Single channel kinetics

In the absence of channel-block, both open- and burst-time distributions were usually described by a single exponential, revealing the presence of one open-state. The mean open-times were only modestly voltage-sensitive and increased from 0.7 ms at +75 mV to 1.4 ms at -75 mV, due to a reduction in the channel closing rate constant α; this corresponds to an e-fold reduction for every 213 mV. Although such a voltage-sensitive reduction in the closing rate constant is also a feature of vertebrate nicotinic AChR channels, they are more sensitive with an e-fold reduction every 78 mV for skeletal muscle receptors (for example see Colquhoun & Ogden, 1988), and an e-fold reduction for every 156 mV for the ganglionic receptors (for example see Mathie *et al.*, 1990).

The closed-time distributions were more complex and were described by the sum of two or three exponential components, revealing at least two closed states. In general these closed events could be classified as short 'within-activation' and long 'between-activation' closures. Neither component exhibited any appreciable voltage-dependence.

Channel-block at positive potentials

At positive holding potentials a fast flickering open channel-block was observed in the presence of high concentrations (>60 μM) of morantel. The voltage-sensitivity of the blocking rate, k_{+B} predicted an e-fold increase for every 44 mV negative shift in holding potential and a value for the relative electrical distance for a single morantel block site of 1.1. This is inconsistent with a single block site within the channel pore for a monovalent cation, such as morantel. Further inconsistencies with the predictions of simple bimolecular channel-block included the slopes of frequency block plots and the finding that the burst length appeared independent of morantel concentration.

Channel-block at negative holding potentials

A more complex form of open channel-block was clearly present at negative holding potentials and comprised two identifiable block durations: one whose duration was short ($\sim$13 ms) and independent of morantel concentration and another whose duration was long and increased in a concentration-dependent manner (up to minutes). These two components conspired to produce a marked reduction in the probability of channel opening with increasing morantel concentration. This relationship could not be described assuming simple channel-block; when the data were fitted to the Hill equation, the best fit was obtained with a Hill coefficient of 1.6, suggesting positive cooperativity between at least two blocking molecules. The suggestion that there is more than one block site in the ion pore for large organic molecules is not novel (Adelman & French, 1978; Davies *et al.*, 1989; Gingrich *et al.*, 1993; Maconochie & Steinbach, 1995) and cooperative multi-ion block of channels by simple ions is well recognized (for discussion see Hille, 1992). In the present investigation we used a minimal sequential double block model that describes such a cooperative interaction (Results). The model requires that the occupation of a binding site, MB1, near the mouth of the channel pore precedes binding to the second site, MB2, deeper within the pore. It allows MB1 and MB2 to be occupied simultaneously but does not allow a molecule at MB2 to leave the channel when MB1 is occupied. Thus as the concentration of morantel increases the occupation of MB1 increases so that there is a concentration-dependent increase in the duration of the occupation of the MB2 site.

The nicotinic AChR appears to have multiple binding sites for channel-blocking molecules: quinacrine azide, a derivative of a channel-blocker photoaffinity labels an M1 region believed

to form part of the 25–30 A° funnel entrance of the open channel (Dipaola *et al.*, 1990); $TPMP^+$ photoaffinity labels an MII region of the pore that appears to be the QX 222 blocking site (Hucho *et al.*, 1986). If we consider the large size of the extracellular antrum of the vertebrate nicotinic AChR pore (Zhorov *et al.*, 1991), the existence of more than one binding site for a blocking molecule is quite plausible. It is tempting to suggest that a site equivalent to the outer 20' region in the MII region of the pore (Lester, 1992) may represent the MB1 site and the QX 222 binding site (the 10' hydrophobic ring and 6' anionic ring on the inner MII region of the pore, Galzi *et al.*, 1991; Lester, 1992), may represent the MB2 block site.

Values of rate constants estimated from the sequence of open- and closed-times also supports the sequential double block model

Horn and Lange (1983) have described a technique for the estimation of rate constants for any kinetic scheme, by fitting the parameters of the hypothesized Q matrix of the model to the entire sequence of open and closed dwell times by maximum likelihood. We also tested this approach to estimate directly the rate of constants of our block model from records showing only one active channel. The techniques of Colquhoun and Hawkes (1977, 1981) were used to make these estimates and programs written in FORTRAN using conditional probability density functions, of the form described in equation 1. It has been pointed out by Fredkin and Rice (1992), that this sort of approach may be successful for complicated schemes but sometimes fails for simple models. Apparently reliable estimation rate constants is particularly difficult when the closed-states are not well separated, because there is an inherent ambiguity in the closed-state kinetics due to aggregation. We chose the 100 μM concentration results at −75 mV, because this was the concentration where we consistently separated both the short, and long, block durations from the normal channel closures.

Table 4 shows the mean and s.e.mean values obtained for the rate constants of the model at −75 mV. The striking feature of these results is the similarity to those results obtained from the *Po* least squares estimates. For example the maximum likelihood estimates gave values of 1.5 μM for K_B, 24 s^{-1} for k_B, 57 s^{-1} for γ, 51 s^{-1} for δ and 1.6 μM for $K_{B'}$: these values compare with 1.1 μM for K_B and $K_{B'}$, 21 s^{-1} for k_{-B} and 54 s^{-1} for γ and δ obtained from the least squares estimation. The similar estimates for the dissociation constants, K_B and K'_B, obtained by both methods, lends support for the use of our simple sequential double block model. We also checked the predictions of the model and found that the estimated rate constants predicted the concentration-dependence of *Po*, the Hill coefficient, as well as the probability density functions of the open and closed-times for 100 μM morantel (data not shown).

Table 4 Rate constants estimated by maximum likelihood for the sequential multi-ion channel-block model from the sequence of open- and closed- times with 100 μM morantel and at −75 mV

β'	α	k_{+B}	k_{-B}	γ	δ	k'_{+B}	k'_{-B}
3.14 ±0.70	1144 ±160	16.1 ±2.3	23.7 ±4.0	56.7 ±20.1	51.3 ±13.2	29.1 ±7.3	47.6 ±16.0

Data shown are means ± s.e.mean, $n=4$. Note that $K_B = k_{-B}/k_{+B} = 1.47$ μM; $K'_B = k'_{-B}/k'_{+B} = 1.64$ μM; $\gamma/\delta = 1.1$. Units are s^{-1} except for k_{+B} and k'_{+B} which are $\mu M^{-1}s^{-1}$.

Other processes used to explain deviations from the predictions of simple open channel-block

One alternative explanation of our findings is that of desensitization. It is likely that desensitization in general is a phenomena associated with high agonist concentrations and results from long-lived shut states which have the agonist binding sites occupied. At vertebrate nicotinic AChR the channel openings during desensitization are seen as clusters separated by long closed-times which may have mean durations as long as 34 s (Sakmann *et al.*, 1980; Colquhoun & Ogden, 1988). Such long-lived desensitized states could explain our observations if they occurred only at negative potentials and were concentration-dependent in duration. However, when observed in vertebrate and *Ascaris* preparations, these long desensitized/closed-times are essentially not voltage-sensitive (Colquhoun & Ogden, 1988; Robertson & Martin, 1993a). Moreover when present, voltage-sensitive desensitization appears to be Ca^{2+}-dependent and supported by depolarization of the cell membrane (Manthey, 1966, 1970; Mildei, 1980). The Ca^{2+} concentration of our solutions was deliberately low to minimize any Ca^{2+}-dependent changes in single-channel activity. In addition, the long concentration- and voltage-dependent gaps in single-channel records obtained with morantel as the agonist did not increase in frequency with the passage of time as they are expected to do if they were explained by desensitization.

We also estimated, from our data, rate constants for a sequential model (C↔O↔B↔D) in which the blocked channel (B) could enter a desensitized state (D) and found that the mean duration of the desensitized state would have to be voltage-dependent and concentration-dependent to explain our data. If desensitization were the explanation for the long block periods at negative potentials, then the duration of the desensitized state would be expected to have the same mean duration (it did not) throughout the concentration range, 10–100 μM morantel, where the *Po* plot (Figure 3a) indicates receptor saturation. For these reasons we believe that the voltage-sensitive and concentration-dependent long gaps seen at negative potentials in this study cannot be explained by desensitization.

One further alternative explanation of our findings could lie in the presence of a closed-trapped-blocked state (Gurney & Rang, 1984). Ogden & Colquhoun (1988) have discussed in some detail the implications of such mechanisms, which could result in a concentration-dependent reduction in mean burst length but which still predict a linear relationship between the reciprocal mean open-times and the concentration of the blocking molecule. However the presence of concentration-dependent and voltage-sensitive long-block durations are not readily explained by models encompassing a closed-trapped-blocked state, which would predict a concentration-independent gap duration.

Conclusion

We have observed that morantel both opens and blocks the nitotinic AChR in the somatic muscle cells of *Ascaris*. The mechanism of block appears complex showing cooperativity and may be explained by the presence of two block sites within the channel pore. The marked voltage-sensitivity and bell-shaped concentration-dependence of macroscopic currents produced by morantel (Harrow & Gration, 1985) may be explained by the behaviour of the channel currents seen in this study.

This work was sponsored by the Wellcome Trust. We would like to thank Dr D.C. Ogden and Dr M.B. Cannell for reading the manuscript and for a helpful discussion of our findings.

References

ADAMS, P.R. (1976). Drug blockade of open end-plate channels. *J. Physiol.*, **260**, 531–552.

ADELMAN, W.J. & FRENCH, R.J. (1978). Blocking of squid axon potassium channel by external caesium ions. *J. Physiol.*, **276**, 13–25.

BALDWIN, E. & MOYLE, V. (1949). A contribution to the physiology and pharmacology of *Ascaris lumbricoides* from the pig. *Br. J. Pharmacol.*, **4**, 145–152.

COLQUHOUN, D. & HAWKES, A.G. (1977). Relaxation and fluctuations of membrane currents that flow through drug-operated channels. *Proc. R. Soc. (Lond.)*, **B199**, 231–262.

COLQUHOUN, D. & HAWKES, A.G. (1981). On the stochastic properties of single ion channels. *Proc. R. Soc. (Lond.)*, **B211**, 205–235.

COLQUHOUN, D & OGDEN, D.C. (1988). Activation of ion channels in the frog end-plate by high concentrations of acetylcholine. *J. Physiol.*, **395**, 131–159.

COLQUHOUN, D. & SAKMANN, B. (1985). Fast events in single-channel currents activated by acetylcholine and its analogues at the frog muscle end-plate. *J. Physiol.*, **369**, 501–557.

COLQUHOUN, D. & SIGWORTH, F.J. (1983). Fitting and statistical analysis of single-channel records. In *Single-channel Recording*, ed. Sakmann, B. & Neher, E., pp. 191–263. New York: Plenum Press.

DAVIES, N.W., SPRUCE, A.E., STANDEN, N.B. & STANFIELD, P.R. (1989). Multiple blocking mechanisms of ATP-sensitive potassium channels of frog skeletal muscle by tetra-ethylammonium ions. *J. Physiol.*, **413**, 31–48.

DEL CASTILLO, J., DE MELLO, W.C. & MORALES, T. (1963). The physiological role of acetylcholine in the neuromuscular system of *Ascaris lumbricoides*. *Arch. Internat. Physiol. Biochimie*, **71**, 741–757.

DIPAOLA, M., KAO, P.N. & KARLIN, A. (1990). Mapping the -subunit site photolabelled by the non-competitive inhibitor (3H)quinacrine azide in the active state of the nicotinic acetylcholine receptor. *J. Biol. Chem.*, **265**, 11017–11029.

EVANS, A.M. & MARTIN, R.J. (1992a). The cationic agonist blocks nicotinic acetylcholine channels from *Ascaris suum* at positive potentials. *J. Physiol.*, **459**, 394P.

EVANS, A.M. & MARTIN, R.J. (1992b). Morantel may bind to more than one site within nicotinic acetylcholine channels from *Ascaris suum*. *J. Physiol.*, **459**, 489P.

EVANS, A.M. & MARTIN, R.J. (1993a). On the block by morantel of nicotinic acetylcholine channels isolated from *Ascaris suum*: positive cooperativity between at least two blocking molecules. *J. Physiol.*, **467**, 171P.

EVANS, A.M. & MARTIN, R.J. (1993b). On the block by morantel of nicotinic acetylcholine receptors isolated from *Ascaris suum*: rate constants for multi-ion block estimated by maximum likelihood. *J. Physiol.*, **467**, 254P.

FREDKIN, D.R. & RICE, J.A. (1992). Maximum likelihood estimation and identification directly from single-channel recordings. *Proc. R. Soc. (Lond.)*, **B294**, 125–132.

GALZI, J., REVAH, F., BESSIS, A. & CHANGEUX, J. (1991). Functional architecture of the nicotinic acetylcholine receptor: from electric organ to brain. *Ann. Rev. Pharmacol.*, **31**, 37–72.

GINGRICH, B.J., BEARDSLEY, D. & YUE, D.T. (1993). Ultra-deep blockade of Na^+ channels by a quaternary ammonium ion: catalysis by a transition-intermediate state? *J. Physiol.*, **471**, 319–341.

GURNEY, A.M. & RANG H.P. (1984). The channel-blocking action of methonium compounds on rat submandibular ganglion cells. *Br. J. Pharmacol.*, **82**, 623–642.

HAMILL, O.P., MARTY, A., NEHER, E., SAKMANN, B. & SIGWORTH, F.J. (1981). Improved patch-clamp techniques for high-resolution current recording from cells and cell-free membrane patches. *Pflügers Archiv.*, **391**, 85–100.

HARROW, I.D. & GRATION, K.A.F. (1985). Mode of action of the anthelmintics morantel, pyrantel and levamisole on the muscle cell membrane of the nematode *Ascaris suum*. *Pest Sci.*, **16**, 662–672.

HORN, D. & LANGE, K. (1983). Estimating kinetic constants from single channel data. *Biophysics J.*, **43**, 207–223.

HILLE, B. (1992). *Ionic Channels of Excitable Membranes*. Second Edition. pp. 390–422. Sunderland, Massachusetts: Sinauer Associates Inc.

HUCHO, F., OBERTHUR, W. & LOTTSPEICH, F. (1986). The ion channel of the nicotinic acetylcholine receptor is formed by the homologous helices MII of the receptor subunits. *FEBS Letts.*, **205**, 137–142.

IMOTO, K., BUSCH, C., SAKMANN, B., MISHINA, M., KONNO, T., NAKAI, J., BUJO, H., MORI, Y., FUKUDA, K. & NUMA, S. (1988). Rings of negatively charged amino acids determine the acetylcholine receptor channel conductance. *Nature*, **335**, 645–648.

LESTER, H.A. (1992). The permeation pathway of neuromuscular-gated ion channels. *Ann. Rev. Biophys. Biomol. Struct.*, **21**, 267–293.

MACONOCHIE, D.J. & STEINBACH, J.H. (1995). Block by acetylcholine of mouse muscle nicotinic receptors, stabley expressed in fibroblasts. *J. Gen. Physiol.*, **106**, 113–147.

MANTHEY, A.A. (1966). The effect of calcium on desensitisation of membrane receptors at the neuromuscular junction. *J. Gen. Physiol.*, **49**, 963–976.

MANTHEY, A.A. (1970). Further studies on the effect of calcium on the time course of action of carbamyl choline at the neuromuscular junction. *J. Gen. Physiol.*, **56**, 407–419.

MARTIN, R.J. (1982). Electrophysiological effects of piperazine and diethylcarbamazine on *Ascaris suum* somatic muscle. *Br. J. Pharmacol.*, **77**, 255–265.

MARTIN, R.J., KUSEL, J.R. & PENNINGTON, A.J. (1990). Surface properties of membrane vesicles prepared from muscle cells of *Ascaris suum*. *J. Parasitol.*, **76**, 340–348.

MARTIN, R.J., PENNINGTON, A.J., DUITTOZ, A.H., ROBERTSON, S. & KUSEL, J.R. (1991). The physiology and pharmacology of neuromuscular transmission in the nematode parasite *Ascaris suum*. *Parasitology*, **102**, S41–S58.

MATHIE, A., COLQUHOUN, D. & CULL-CANDY, S.G. (1990). Rectification of currents activated by nicotinic acetylcholine receptors in rat sympathetic ganglion neurones. *J. Physiol.*, **427**, 625–655.

MILEDI, R. (1980). Intracellular calcium and desensitisation of acetylcholine receptors. *Proc. R. Soc. (Lond.)*, **209**, 447–452.

NATOFF, I.L. (1969). The pharmacology of cholinoceptors in muscle preparations of *Ascaris lumbricoides* var. *suum*. *Br. J. Pharmacol.*, **37**, 251–257.

NEHER, E. & STEINBACH, J.H. (1978). Local anaesthetics transiently block currents through single acetylcholine receptor channels. *J. Physiol.*, **277**, 153–176.

OGDEN, D.C. & COLQUHOUN, D. (1985). Ion channel-block by acetylcholine, carbachol and suberyldicholine at the frog neuromuscular junction. *Proc. R. Soc. (Lond.)*, **B225**, 329–355.

PATLAK, J.B. (1988). Sodium channel sub-conductance levels measured with a new variance-mean analysis. *J. Gen. Physiol.*, **92**, 412–430.

PENNINGTON, A.J. & MARTIN, R.J. (1990). A patch-clamp study of acetylcholine-activated ion channels in *Ascaris suum* muscle. *J. Exp. Biol.*, **154**, 201–221.

ROBERTSON, S.J. & MARTIN, R.J. (1993a). Levamisole-activated single-channel currents from muscle of the nematode parasite *Ascaris suum*. *Br. J. Pharmacol.*, **108**, 170–178.

ROBERTSON, S.J. & MARTIN, R.J. (1993b). The application of levamisole, either to the extracellular or cytoplasmic surface, activates nicotinic single channels in membranes of the nematode parasite *Ascaris suum*. *Pest. Sci.*, **37**, 293–299.

ROZHOVA, E.K., MALYUTINA, T.A. & SHISHOVA, B.A. (1980). Pharmacological characteristics of cholinoreception in somatic muscle of the nematode *Ascaris suum*. *Gen. Pharmacol.*, **11**, 141–146.

SAKMANN, B.J., PATLAK, J. & NEHER, E. (1980). Single acetylcholine-activated channels show burst-kinetics in the presence of desensitizing concentrations of agonist. *Nature*, **286**, 71–73.

TOSCANO RICO, J. (1926). Sur la sensibilite de l'Ascaris a l'action de quelques drogues. *Compte Rendu Seances Soc. Biol.*, **94**, 921–923.

ZHOROV, B.S., BROVTSYNA, N.B., GMIRO, V.E., LUKOMSKAYA, N.Y., SERDYUK, S.E., POTARYEVA, N.N., MAGAZANIK, L.G., KURENNITY, D.E. & SKOK, V.I. (1991). Dimensions of the ion channel in neuronal nicotinic acetylcholine receptor as estimated from analysis of the conformation-activity relationships of open channel-blocking drugs. *J. Memb. Biol.*, **121**, 119–132.

(Received October 10, 1995
Revised March 7, 1996
Accepted March 11, 1996)